



REVIEW

**Formic acid oxidation at platinum–bismuth catalysts\***

KSENIJA Đ. POPOVIĆ\*# and JELENA D. LOVIĆ#

*ICTM – Institute of Electrochemistry, University of Belgrade, Njegoševa 12, P. O. Box 473,  
11000 Belgrade, Serbia*

(Received 18 March, revised 24 April, accepted 5 May 2015)

**Abstract:** The field of heterogeneous catalysis, specifically catalysis on bimetallic surfaces, has seen many advances over the past few decades. Bimetallic catalysts, which often show electronic and chemical properties that are distinct from those of their parent metals, offer the opportunity to obtain new catalysts with enhanced selectivity, activity, and stability. The oxidation of formic acid is of permanent interest as a model reaction for the mechanistic understanding of the electro-oxidation of small organic molecules and because of its technical relevance for fuel cell applications. Platinum is one of the most commonly used catalysts for this reaction, despite the fact that it shows a few significant disadvantages, such as high cost and extreme susceptibility to poisoning by CO. To solve these problems, several approaches have been used, but generally, they all consist in the modification of platinum with a second element. Especially, bismuth has received significant attention as a Pt modifier. According to the results presented in this review dealing with the effects influencing formic acid oxidation, it was found that two types of Pt–Bi bimetallic catalysts (bulk and low loading deposits on GC) showed superior catalytic activity in terms of lower onset potentials and oxidation current densities, as well as exceptional stability compared to Pt. The findings in this report are important for an understanding of the mechanism of formic acid electro-oxidation on the bulk alloy and decorated surface, for the development of advanced anode catalysts for direct formic acid fuel cells, as well as for the synthesis of novel low-loading bimetallic catalysts. The use of bimetallic compounds as anode catalysts is an effective solution to overcoming the problems of current stability in the oxidation of formic acid during long-term applications. In the future, the tolerance of both CO poisoning and electrochemical leaching should be considered as the key factors in the development of electrocatalysts for anodic reactions.

**Keywords:** formic acid oxidation; Pt–Bi catalysts; alloy; metal clusters; fuel cell anode catalysts.

\* In memory to Dr Rade M. Stevanović, our friend and colleague.

\* Corresponding author. E-mail: ksenija@tmf.bg.ac.rs

# Serbian Chemical Society member.

doi: 10.2298/JSC150318044P



## CONTENTS

1. INTRODUCTION
2. BULK CATALYSTS FOR ELECTRO-OXIDATION OF FORMIC ACID
  - 2.1. *Activity of bulk catalyst*
    - 2.1.1. Platinum electrodes
    - 2.1.2. Effect of Bi adatoms
    - 2.1.3. PtBi ordered intermetallic compounds
    - 2.1.4. PtBi alloys
  - 2.2. *Stability of bulk catalysts*
3. LOW-LOADING Pt–Bi CATALYSTS
  - 3.1. *Activity of low-loading catalysts*
    - 3.1.1. Pt/GC catalyst
    - 3.1.2. Pt@Bi/GC clusters
  - 3.2. *Stability of low-loading catalysts*
  - 3.3. *Pt(Bi)/GC shell–core catalyst*
4. CONCLUSIONS

## 1. INTRODUCTION

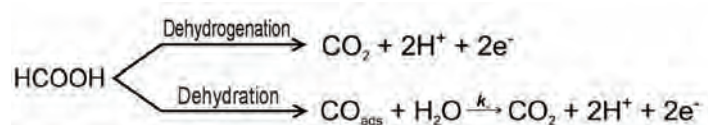
For many years, much attention has been focused on low-temperature fuel cells with energy conversion based on the electrocatalytic oxidation of small organic molecules, such as methanol, ethanol and formic acid. The fuel cell industry has focused the majority of its research on the development of cost-effective, reactive, and durable catalysts.

Electrochemical oxidation of formic acid is under comprehensive investigation for two main reasons: formic acid can be used as a fuel in direct formic acid fuel cell (DFAFC) and can serve as a model reaction that provides a simplified example of the oxidation of more complex organic molecules that can also be used for this purpose.<sup>1</sup> A direct formic acid–oxygen fuel cell with a polymer electrolyte membrane (PEM) has some advantages over a direct methanol fuel cell. Oxidation of formic acid commences at a lower positive potential than methanol oxidation and the crossover of formic acid through the polymer membrane is lower than that of methanol.<sup>2,3</sup> Moreover, formic acid is a relatively benign and non-explosive fuel, which makes it facile in handling and distribution, as compared to hydrogen. On the other hand, it has a lower energy content with respect to hydrogen or methanol. Recent data showed, however, that formic acid fuel cells are attractive alternatives for small portable fuel cell applications.<sup>4,5</sup>

Electrochemical oxidation of formic acid has been widely studied on different metal electrodes. Among them, platinum was shown to exhibit the highest catalytic activity of all the pure metals. This reaction has been investigated at platinum since the early work of Breiter<sup>6</sup> and the results were reviewed by Par-

sons and Van der Noot<sup>1</sup>, and Jarvi and Stuve.<sup>7</sup> Many results have been reported concerning the electrocatalytic oxidation of formic acid from the fundamental viewpoint<sup>8–12</sup> in contrast to the limited information on the properties of formic acid as a fuel. However, in the last few years, this reaction has attracted more attention.<sup>13,14</sup>

As already mentioned above, formic acid oxidation on platinum is considered as a model reaction in electrocatalysis, because the oxidation of formic acid is a simple structure-sensitive process. In spite of the apparent simplicity of the process, that is, the oxidation only requires the elimination of two hydrogen atoms in the form of protons and the transfer of the two corresponding electrons, the oxidation mechanism has a double pathway. Thus, the oxidation of formic acid on Pt electrodes follows the dual path mechanism introduced by Capon and Parsons,<sup>15,16</sup> involving a direct path (dehydrogenation) and an indirect path (dehydration), both generating CO<sub>2</sub> as the final reaction product. This finding was later confirmed by differential electrochemical mass spectrometry (DEMS) measurements.<sup>3</sup> Both routes are structure sensitive and there is a clear dependence of the reactivity on the surface structure, as experiments with single crystal electrodes revealed.<sup>17–21</sup>



In the direct path, formic acid is oxidized through a reactive intermediate to CO<sub>2</sub>, while in the indirect path, formic acid is first dehydrated to the adsorbed CO intermediate, as a poisoning species that hinders the direct reaction path, followed by oxidation of the adsorbed CO by OH formed at higher potentials.

The direct path that proceeds through an active intermediate is the simplest one. Formic acid adsorbs on the surface, probably transferring one electron, to form an active intermediate, and then this intermediate is oxidized to CO<sub>2</sub>. Regarding the nature of the active intermediate, the question is not yet fully resolved.<sup>22–24</sup> Adsorbed formate (HCOO), rather than the formic acid fragment (COOH), was proposed as the reactive intermediate<sup>23,25–27</sup> and this assumption was confirmed by direct surface-enhanced infrared absorption spectroscopy (SEIRAS).<sup>28</sup>

In the indirect pathway, the first step is a dehydration step with the loss of an oxygen atom to form adsorbed CO, which was detected by IR spectroscopy.<sup>10,29</sup> CO adsorbs strongly on the surface, and for this reason, the route is also known as the poisoning route. Thus, adsorbed CO blocks the active sites on the surface and prevents the reaction from proceeding. Accordingly, the catalytic performance of Pt is significantly reduced at low potentials due to CO poisoning.

However, besides being a poisoning species, CO may act as a reactive intermediate, whereby some fraction of  $\text{CO}_{\text{ads}}$  can be oxidized with  $\text{OH}_{\text{ads}}$  to produce  $\text{CO}_2$ .<sup>12</sup>

Nevertheless, platinum is an unavoidable material and considered as one of the most efficient catalysts for the oxidation of small organic molecules but, on the other hand, has several significant disadvantages: high cost and extreme susceptibility to poisoning due to strongly adsorbed intermediates, which are formed during the oxidation processes.<sup>30</sup> Taking this into account, the ideal electrocatalysts would be one that accelerates the direct route and prevents the formation of CO.

It is now well known that these requirements are fulfilled by bimetallic catalysts, which often show electronic and chemical properties that are distinct from those of their constituent metals and offer the chance to obtain new catalysts with enhanced selectivity, activity and stability.

Several approaches have been taken to achieve these goals, but in general, they consist of the modification of platinum with a second element. This modification is usually realized by alloying or by modification of the Pt surface with adsorbed foreign metals in an amount less than a full monolayer.<sup>31,32</sup> The presence of a foreign metal alters the properties of Pt in the bimetallic surfaces.<sup>12,33</sup> The effects of these atoms can be classified in three main categories: electronic, bifunctional and third body effects. The first one, which involves ligand and strain effects, relates to a change in the electronic properties of the catalytically active material. The bifunctional effect is present when the second metal becomes the source of the oxygen required for the oxidation of the fuel. The third body effect implies a change in the distribution of the active adsorption sites due to dilution of the catalytically active material. Generally, more than one of these factors controls the enhanced properties of bimetallic surfaces making separation of the individual contributions difficult.

In order to improve Pt electrocatalytic activity towards HCOOH oxidation and tolerance to CO, addition of metals such as Ru, Pb, Os, Li, Pd, Fe, Bi *etc.*<sup>12,34–39</sup> were applied. Especially, bismuth has received significant attention as a Pt-modifier,<sup>18,31,32,40,41</sup> and different systems, such as PtBi intermetallics,<sup>42–46</sup> PtBi alloys,<sup>39,47,48</sup> electrochemically co-deposited carbon supported PtBi (PtBi/C),<sup>49</sup> or Pt modified by Bi either by underpotential deposition (UPD) or irreversible adsorption<sup>50,51</sup> were proposed as good catalysts for formic acid oxidation.

Besides the many methods for the synthesis of bimetallic catalysts, a new method for the preparation of noble metal coatings was recently proposed. This procedure includes the replacement of the surface layer of a less precious metal (Ru, Cu, Pb and Ti) with a more noble metal (Pt and Pd) by spontaneous electroless exchange upon immersion into a complex solution of Pt or Pd ions.<sup>52,53</sup>

An additional approach for the formation of low dimensional systems is electro-deposition of mono or multilayer metals on different substrates.<sup>54–56</sup> This concept of bimetallic mono and multilayer catalysts has received much attention regarding its possibility to reduce the noble metal quantity and maintain the activity by replacing the under-layer (bulk of the catalyst) with a less noble metal. Moreover, unlike other bimetallic catalysts where the second metal is either in the form of an adatom or as a component of a surface alloy, this type of catalyst allows the study of the electronic effect of the second metal under-layer on the noble catalyst over-layer, as the only operating factor.

In addition, from a practical point of view, long-term stability of the investigated catalysts for formic acid oxidation is very important. Therefore, it is necessary to determine which of the factors mostly affected the improvement of the formic acid oxidation rate and the stability of the catalyst.

In this paper, recent advances in HCOOH oxidation research are presented with focus on the progresses that have been made on Pt–Bi catalysts for the possible use in DFAFCs. Different preparation methods were employed to adapt the properties of Pt. Each method will be emphasized for its advantage and discussed in terms of its limitations, based on the physicochemical and electrochemical characterizations of the catalysts in order to explain the mechanism of action of bismuth added to platinum, the importance of surface composition and surface morphology for the reaction of formic acid oxidation.

## 2. BULK CATALYSTS FOR ELECTRO-OXIDATION OF FORMIC ACID

### 2.1. Activity of bulk catalysts

#### 2.1.1. Platinum electrodes

Platinum, the most studied catalyst for formic acid oxidation, is very susceptible to poisoning species, which significantly reduces its catalytic performance at low potentials, as is well known from the literature.<sup>12</sup> Traditional single crystals represent an ideal model surfaces for the oxidation reaction of small organic molecule and are suitable for surface characterization methods both *in situ* and *ex situ*. Studies on single crystal Pt samples showed that formic acid oxidation is a strongly structure sensitive reaction. The most complete study on formic acid structure sensitivity was realized by the Motoo group,<sup>57</sup> using a complete series of stepped surfaces around the stereographic triangle. The studies of this reaction on stepped Pt surfaces were performed in order to clarify how exactly the step density influences this reaction, *i.e.* higher index or stepped surfaces were used to verify the active site assumption, whether low coordination sites are particularly active. The less poisoned surface was Pt(111), as indicated by the low observed hysteresis, but the activity toward formic acid oxidation was low. It should be noted that the presence of defects, especially on (100) steps, considerably increased the activity of a Pt(111) electrode. For example, in order

to achieve higher rates at moderate poisoning, electrodes having 5–6 atoms wide (111) terraces were the best under the experimental conditions used.

The oxidation of formic acid is a structure sensitive reaction, which implies the existence of adsorption steps in the process. In an electrochemical environment, the adsorption processes have to be considered as complex steps since they always involve the competitive adsorption of anions, water and/or hydrogen, which can have different dependences on concentration, and affects the relative rates of dissociative adsorption in a complex way.<sup>21</sup>

These kind of studies are relevant not only from a fundamental point of view but also from a practical one, because in practical applications, the stepped surfaces may be considered as models for surface defects always present on polycrystalline electrodes.

Remembering that the cyclic voltammogram for an as-prepared polycrystalline Pt electrode (Fig. 1a) is described by a region of hydrogen adsorption/desorption ( $E < 0.05$  V vs. SCE), separated by a double layer from the region of surface oxide formation ( $E > 0.45$  V vs. SCE). The absence of well-developed peaks at an as-prepared Pt polycrystalline electrode in the hydrogen adsorption/desorption region is caused by the employed preparation procedure.

The activity of Pt electrode towards formic acid oxidation is given in Fig. 2a. The cyclic voltammogram shows a well-established feature for formic acid oxidation.<sup>7</sup> In the forward scan, the current slowly increases reaching a plateau at  $\approx 0.25$  V vs. SCE followed by an ascending current starting at 0.5 V vs. SCE, which attains a maximum at  $\approx 0.62$  V vs. SCE. Such behavior could be explained considering the dual path mechanism, *i.e.*, dehydrogenation assigned as the direct path, based on the oxidation of formate,<sup>28</sup> and dehydration, indirect path, assumes the formation of CO<sub>ads</sub>, both generate CO<sub>2</sub> as the final reaction product. At low potentials, HCOOH oxidizes through the direct path with the simultaneous formation of CO<sub>ads</sub>. Increasing coverage with CO<sub>ads</sub> reduces the Pt sites available for the direct path and current slowly increases reaching a plateau. Subsequent formation of oxygen-containing species on Pt enables the oxidative removal of CO<sub>ads</sub>, more Pt sites become available for HCOOH oxidation and current increases until Pt oxide, inactive for HCOOH oxidation, is formed, which results in a current peak at  $\approx 0.62$  V vs. SCE. In the backward scan, the sharp increase in the HCOOH oxidation current coincides with the reduction of Pt oxide. The currents are much higher than in the forward sweep, because the Pt surface is freed of CO<sub>ads</sub>.

### 2.1.2. Effect of Bi adatoms

The addition of foreign metals to Pt surfaces in amounts less than a full monolayer results in modified surface catalytic properties. Therefore, surfaces of bimetallic electrodes often show improved electrocatalytic behavior. It was reported in earlier studies that Bi modification of platinum electrodes could exceptionally increase their reactivity toward HCOOH oxidation, depending on the

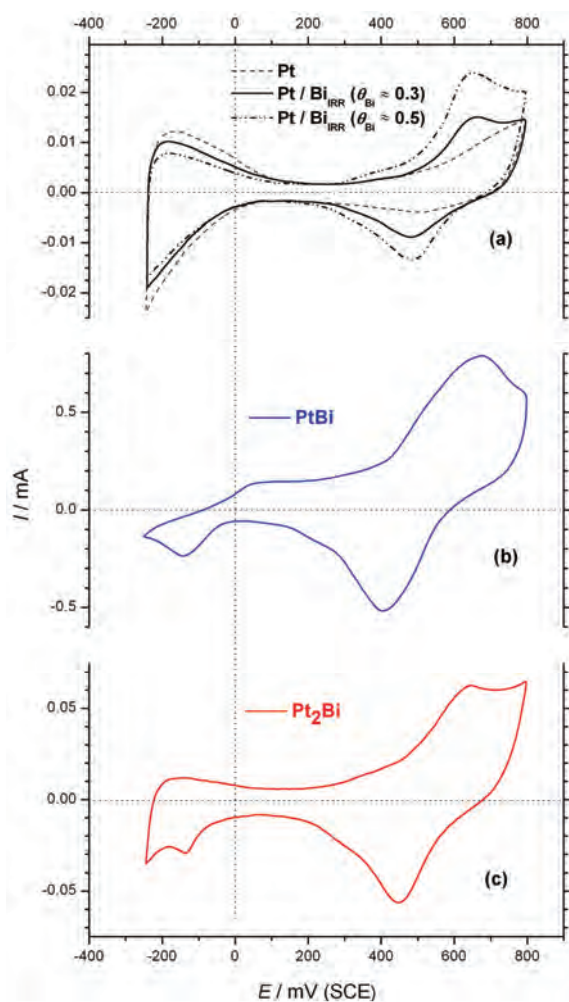


Fig. 1. Basic voltammograms for Pt and Pt/Bi<sub>IRR</sub> (a), PtBi alloy (b) and Pt<sub>2</sub>Bi (c) bulk electrodes in 0.1 M H<sub>2</sub>SO<sub>4</sub>. Scan rate: 50 mV s<sup>-1</sup>.  $\omega = 1500$  rpm.  $T = 295$  K.

Bi surface coverage.<sup>40,47</sup> Most current studies exploring structure/property/activity relationships based on experimental approaches either use well-defined single crystals as a model or are based on modified noble single crystal surfaces. Feliu and co-workers<sup>58,59</sup> as well as Abruna and co-workers<sup>60,61</sup> reported that bismuth-modified platinum low and high-index single crystal surfaces, which were prepared *via* the under-potential deposition (UPD) process, exhibited extraordinary enhancement in reactivity towards formic acid oxidation.

Irreversibly adsorbed Bi<sup>40,47,51,62</sup> inhibits poison formation simultaneously enhancing dehydrogenation,<sup>51</sup> *i.e.*, this modification is an efficient way to hinder the dehydration path (CO-intermediate pathway) in favor of the direct path.<sup>63</sup> This increased selectivity for dehydrogenation was proposed to be an “ensemble effect”<sup>64,65</sup> in which the adsorbed Bi divides the Pt surface into small domains

where only dehydrogenation can occur. A correlation between ensemble size and formic acid oxidation activity was also established.<sup>66</sup> According to literature data, the activity of Pt catalysts modified with Bi depends on the shape of the Pt nanocrystals,<sup>67</sup> and varies with the size of the particles<sup>68</sup> and the loading of the Pt catalyst.<sup>63</sup>

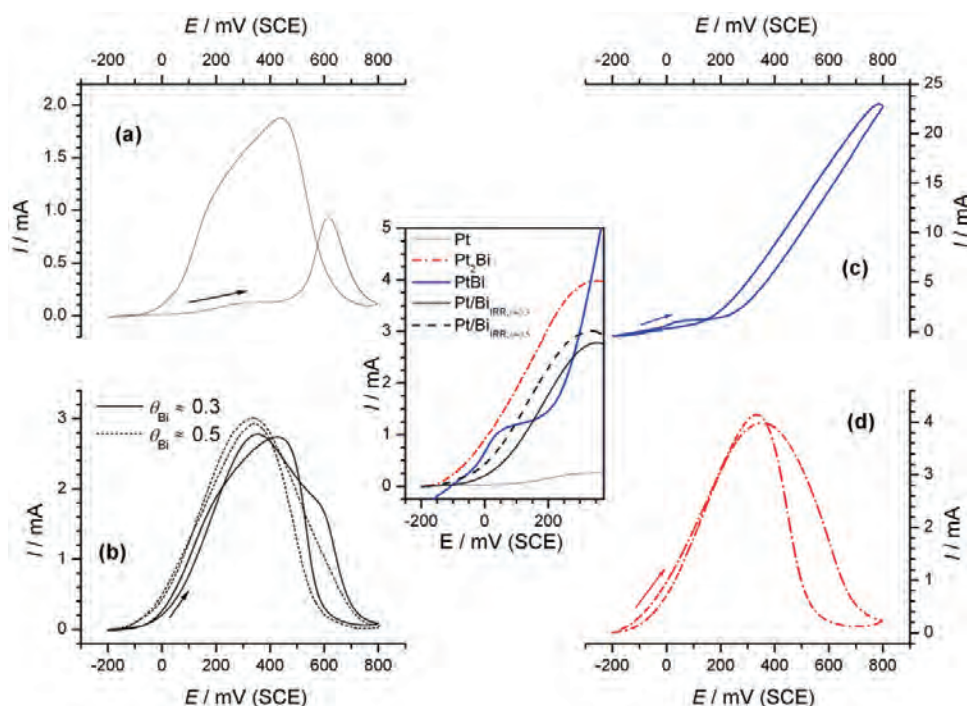


Fig. 2. Cyclic voltammograms for the oxidation of 0.125 M HCOOH in 0.1 M H<sub>2</sub>SO<sub>4</sub> solution on: a) Pt, b) Pt/Bi<sub>IRR</sub>, c) PtBi and d) Pt<sub>2</sub>Bi catalysts. Inset: magnification of the onset potential region. Scan rate: 50 mV s<sup>-1</sup>.  $\omega = 1500$  rpm.  $T = 295$  K.

The beneficial effect of Bi on Pt for this reaction could be due to changes in the Pt–Pt distance that favor the direct route in formic acid oxidation,<sup>69</sup> or to the formation of surface Bi oxides that participate in the oxidation of intermediates,<sup>39,70</sup> or to electronic effects by lowering the electron density of the 5d orbitals, resulting in a considerable decrease of the CO binding strength to Pt,<sup>33,71</sup> or to the ensemble effect creating an appropriate size of Pt domains and thereby providing direct oxidation of HCOOH to CO<sub>2</sub>.<sup>48,64</sup> Depending on the preparation of the catalysts and their resulting surface composition, the contribution of the above effects may vary.

In the research performed by our group,<sup>72</sup> the oxidation of formic acid was studied on polycrystalline Pt modified by irreversibly adsorbed Bi (Pt/Bi<sub>IRR</sub>) (Fig. 2b). The experiments were realized without Bi cations in solution, as



opposed to modification by an UPD metal, thereby avoiding competition between adsorption/reaction steps of the reactant and modifier. The results were contrasted to pure Pt (Fig. 2a). Modification of the Pt electrode was performed at the open circuit potential, as described elsewhere.<sup>65</sup> After modification, the electrode was rinsed with water and transferred into a cell containing supporting electrolyte. The fraction of the sites covered by Bi (denoted Pt/Bi<sub>IRR;θ</sub>) was estimated from the decrease in the charge for desorption of hydrogen, due to the fact that hydrogen does not adsorb on Bi,<sup>73</sup> *i.e.*, only the Pt sites not blocked by Bi were available for hydrogen adsorption. In order to avoid Bi dissolution, the anodic potential limit was set at 0.5 V *vs.* SCE, since it was established that the initial amount of Bi was almost completely retained when the upper potential limit was fixed below 0.75 V *vs.* RHE.<sup>74</sup> This finding is in agreement with that reported using electrochemical quartz crystal microbalance (EQCM) analysis of the Bi oxidation mechanism on smooth Pt electrodes.<sup>75</sup>

The activities of Pt/Bi<sub>IRR</sub> and Pt electrodes towards formic acid oxidation are compared in Fig. 2a and b and the results showed that the onset potential for the reaction on the Pt/Bi<sub>IRR</sub> ( $\theta_{\text{Bi}} \approx 0.3$ ) was about 0.1 V less positive than on the Pt electrode. The current reached a peak that corresponded to the oxidation of HCOOH to CO<sub>2</sub> *via* the direct path, occurring on Pt sites that were not blocked by the poisoning CO<sub>ads</sub> species. On the descending part of the curve, a shoulder appeared at almost the same potential as the peak on the curve for the pure Pt electrode, which arises from the HCOOH oxidation on the sites being freed by CO<sub>ads</sub> oxidation. Thus, HCOOH oxidation on Pt/Bi<sub>IRR;θ≈0.3</sub> proceeded predominantly by the dehydrogenation path with some minor degree of dehydration also occurring.

HCOOH oxidation was also tested on a Pt/Bi<sub>IRR</sub> electrode with larger coverage by Bi ( $\theta_{\text{Bi}} \approx 0.5$ ). Bell-shaped voltammogram clearly suggests that oxidation of HCOOH on this electrode proceeds through dehydrogenation path. It is noticeable that the dehydration path is completely suppressed. The increased selectivity toward the dehydrogenation path on Pt/Bi<sub>IRR</sub> compared to Pt was mainly the result of an ensemble effect caused by Bi reducing the continuous Pt sites necessary for dehydration. Nevertheless, the ensemble effect on the Pt/Bi<sub>IRR</sub> catalyst was enabled by adsorbed Bi, which practically had no influence on the neighboring free Pt atoms.

### 2.1.3. PtBi ordered intermetallic compounds

Recently, Abruna and co-workers<sup>42,43,45,69</sup> studied the electro-oxidation of formic acid on the surface of ordered intermetallic compounds PtBi and PtBi<sub>2</sub>. The choice of PtBi was based on extensive earlier studies in which the enhanced activity of Pt surfaces modified with irreversibly adsorbed Bi adlayers toward the oxidation of formic acid was established.<sup>40,60–62</sup>

Intermetallics are binary or multi-elemental metallic compounds that, since they have well-defined crystalline structures, offer predictable control over structural, geometric, and electronic effects in a manner that is not available when disordered alloys are used. In principle, the electronic and atomic structures, both of which are well known to be important parameters for electrocatalytic activity, can be significantly controlled. As the order in intermetallic phases arises from the high enthalpy of mixing, a high chemical and structural stability could be expected. Therefore, in contrast to disordered alloys, all Pt (and Bi) atoms on the surface of an ordered intermetallic phase have the same local geometry and thus, the same activity.

The results obtained in these studies relating to formic acid oxidation indicated that the PtBi ordered intermetallic phase has properties and reactivity that are dramatically different from those of bare platinum surfaces. Especially, the onset potential for the electrocatalytic oxidation of formic acid is significantly shifted (by over 300 mV) to more negative values and the current density (at a given potential) is significantly enhanced when compared to pure Pt. Moreover, PtBi displayed virtual immunity to CO poisoning.<sup>69</sup> Oana *et al.*<sup>76</sup> found for the intermetallic structures that the susceptibility for CO adsorption on Pt was drastically reduced on PtBi<sub>2</sub> and PtBi surfaces, with respect to Pt, due to an increase in the Fermi level of the system induced by Bi.

According to Abruna and co-workers,<sup>45,69</sup> the origin of the catalytic activity was related to electronic effects enhancing the affinity of PtBi for formic acid adsorption and producing surface oxides at low potentials, as well as to geometric effects that reduces the affinity for CO poisoning. The shift in the onset potential and the increase in the current density are due to electronic effects. In essence, the formation of the PtBi ordered intermetallic results in a charge redistribution (as a first approximation arising from work function differences), which enhances the affinity of PtBi towards formic acid and further gives rise to the formation of surface oxides at much lower potentials. Regarding the geometric effect, contrary to any Pt-based alloy where the Pt–Pt distance for nearest-neighbor Pt atoms is essentially the same as in Pt metal (2.78 Å), in ordered intermetallic compounds, the Pt–Pt distances can be modulated over a range of a factor of 2. For example, in PtBi the Pt–Pt distance in the (001) plane is 4.32 Å. Such distances were expected to diminish significantly CO poisoning, by reducing bridge sites and eliminating 3-fold hollow adsorption sites. However, some electronic effects could also be involved.

Therefore, ordered intermetallic compounds, which were proposed as powerful catalysts for formic acid oxidation,<sup>42–46</sup> not only exhibited greatly enhanced electrocatalytic activity (especially relative to Pt), but they could also serve as model systems to explore structure/composition/property/activity relationships.

#### 2.1.4. PtBi alloys

The fact that formic acid is a good candidate for DFAFCs initiated the study of its oxidation on so-called real catalysts, such as bulk PtBi alloy and two-phase Pt<sub>2</sub>Bi catalysts.<sup>39,48,72</sup>

In one of our previous works, formic acid oxidation was investigated on PtBi alloy samples obtained according to the Bi–Pt phase diagram<sup>39</sup> by melting the pure elements under an inert atmosphere in the proportion of Bi to Pt of 1:1, and the alloy was characterized by X-ray photoelectron spectroscopy (XPS) and by X-ray diffraction (XRD) analysis.<sup>39,48</sup>

XPS analysis revealed three chemical states of Bi, *i.e.*, PtBi or Bi(0), Bi<sub>2</sub>O<sub>3</sub> and BiO(OH) on the catalyst surface (Table I).<sup>39</sup> These results suggested a model in which the PtBi alloy was covered by a layer of Bi<sub>2</sub>O<sub>3</sub> and the very top of this layer contained BiO(OH) species.

TABLE I. XPS analysis of the surface composition of differently treated PtBi 1:1 alloy; BE – the binding energies of the Bi 4f<sub>7/2</sub> excitation; FWHM – the full width at half maximum; take-off angle (90 or 15°) is next to the sample name in brackets<sup>39</sup>

Sample	BE Bi 4f <sub>7/2</sub> , eV	FWHM, eV	Approximate composition, %	Species
Polished electrode	157.3	0.9	34.3	Bi–Pt
	158.8	1.42	65.7	Bi <sup>3+</sup>
Equilibrated at OCP (90°)	157.4	0.9	63.2	Bi–Pt
	158.3	1.6	31.8	Bi <sup>3+</sup>
	159.6	1.9	4.9	BiO(OH)
Equilibrated at OCP (15°)	157.5	1.0	64.7	Bi–Pt
	158.5	1.6	22.0	Bi <sup>3+</sup>
	159.5	1.7	13.3	BiO(OH)
Oxidized at 0.8 V vs. SCE (90°)	157.5	0.9	43.2	Bi–Pt
	158.5	1.3	44.1	Bi <sup>3+</sup>
	159.3	1.8	12.6	BiO(OH)
Oxidized at 0.8 V vs. SCE (15°)	157.8	1.1	34.4	Bi–Pt
	158.8	1.2	51.8	Bi <sup>3+</sup>
	159.6	1.3	13.8	BiO(OH)

XRD characterization of the PtBi alloy was performed to determine its phase composition. The diffraction pattern reveals peaks characteristic for hexagonal structure of the PtBi alloy and very small additional maxima that were assigned to traces of platinum cubic phase ( $\approx 0.7$  wt. %).<sup>48</sup>

Electrochemical characterization showed that PtBi followed the behavior of its constituents.<sup>39</sup> In the potential range up to 0.05 V vs. SCE, the electrode activity and the processes involved were determined by the behavior of pure Bi. It was established that the activity of PtBi was highly dependent on the reduction/oxidation of Bi species. Dissolution of Bi, *i.e.*, leaching from the alloy matrix, proceeded all along the anodic potential scan.<sup>39,42</sup> Comparison of the

basic voltammograms for PtBi and Pt (Fig. 1a and b) showed that the deposition/dissolution of Bi completely suppressed hydrogen adsorption/desorption on Pt, as well as that the surface oxidation on PtBi was initiated at significantly lower positive potentials. The fact that adsorption/desorption of hydrogen was completely suppressed on the PtBi surface, as well as absolute inactivity of both the Bi and PtBi surfaces for the adsorption of CO, made determination of the real surface area impossible. Therefore, comparison of activity was given by the geometric surface area.

The voltammograms for the oxidation of formic acid on Pt and PtBi alloy electrodes, given in Fig. 2a and c, respectively, clearly indicated a dependence of the activity on the reduction/oxidation processes of Bi. Oxidation of formic acid does not occur on pure Bi<sup>39,77</sup> and, consequently, does not occur on PtBi covered by Bi. Hence, the beginning of the reaction must be linked to free Pt sites on the PtBi. Relative to Pt, the onset potential on the PtBi electrode was shifted towards negative potentials by more than 0.25 V and the current densities at 0.05 V vs. SCE were higher by about two and half orders of magnitude.

The exceptional activity of PtBi is caused by UPD phenomena of Bi on Pt, which was electrochemically detected. Namely, after recording the voltammogram for PtBi, this electrode was replaced with Pt and voltammograms were taken in the supporting solution with and without HCOOH. The voltammetric profiles obtained in the supporting solution indicated an underpotential deposition of Bi on Pt, evidencing that dissolved Bi could be adsorbed on Pt sites as an UPD layer. In the presence of formic acid, voltammogram displayed typical features for formic acid oxidation on a Bi-modified Pt surface,<sup>12</sup> clearly suggesting that this reaction on the PtBi alloy occurs on the Bi modified Pt sites on the PtBi surface and the huge increase in catalytic activity relative to polycrystalline Pt was attributed to UPD phenomena of Bi leached from the alloy matrix and re-adsorbed on Pt.

In addition, based on XPS analysis, it is proposed that some contribution of a bifunctional action, enabled by the presence of hydroxylated Bi species, should be taken into consideration.

Our studies of Pt<sub>2</sub>Bi electrode,<sup>48,72</sup> a two-phase material consisting of PtBi alloy and pure Pt, revealed that this is a powerful catalyst for formic acid oxidation. Characterization of the catalyst was realized by XRD spectroscopy (phase composition), STM (surface morphology) and CO<sub>ads</sub> stripping voltammetry (surface composition).

Comparison of the basic voltammograms of Pt<sub>2</sub>Bi electrode and Pt in the potential range up to 0.05 V vs. SCE revealed that the presence of Bi suppressed hydrogen adsorption/desorption to a large extent (Fig. 1c). The cathodic peak at approximately -0.1 V vs. SCE could be correlated to the reduction of Bi oxide species and adsorbed Bi<sup>3+</sup>, species formed in the positive going scan.<sup>39,43</sup> Com-

prehensive oxide formation/reduction was presented by the anodic and cathodic peaks that are superimposed over those of Pt oxide formation and reduction, although the peak position that corresponds to oxide reduction on Pt<sub>2</sub>Bi was slightly shifted towards negative potentials with respect to Pt, indicating some electronic interaction between Pt and Bi. A similar behavior was reported for smooth polycrystalline Pt electrodes in the presence of Bi(III) ions<sup>78</sup> and for PtBi (1:1) alloy.<sup>39</sup>

The cyclic voltammogram for formic acid oxidation on Pt<sub>2</sub>Bi is presented in Fig. 2d. On Pt<sub>2</sub>Bi catalyst, formic acid oxidation commenced more than 0.2 V earlier than on Pt. The currents increased reaching a peak with a current  $\approx 30$  times higher than the plateau on Pt and then diminished up to the positive potential limit. As Bi does not adsorb formic acid,<sup>39,77</sup> the oxidation of formic acid occurred on pure Pt domains and on Pt atoms on PtBi domains. The bell-shaped voltammogram for formic acid oxidation suggests that the reaction on Pt<sub>2</sub>Bi proceeded through the dehydrogenation path with the dehydration path being completely suppressed. Compared to Pt, the high activity of the Pt<sub>2</sub>Bi catalyst could be explained by increased selectivity toward the dehydrogenation path caused by an ensemble effect originating from the interruption of continuous Pt sites by Bi atoms.

CO<sub>ads</sub> stripping voltammetry recorded at Pt<sub>2</sub>Bi and Pt<sup>48</sup> demonstrated that onset potential and the peak position at Pt<sub>2</sub>Bi were slightly shifted to more negative potentials relative to Pt, indicating the presence of some electronic modification of the Pt surface atoms, capable for CO adsorption, by Bi. Since Bi<sup>74</sup> and PtBi<sup>69</sup> are inactive for CO adsorption, the oxidation of CO occurs only on the Pt domains. Therefore, the charge under the CO<sub>ads</sub> peak at Pt<sub>2</sub>Bi reflecting a process at the surface of the Pt phase was used for determining the contribution of pure Pt in the surface composition of the Pt<sub>2</sub>Bi catalyst. The estimated contribution of pure Pt on the Pt<sub>2</sub>Bi surface corresponded closely to bulk composition, thus indicating that adsorbed CO also prevents leaching of Bi.

In order to test whether the surface morphology of Pt<sub>2</sub>Bi changes during formic acid oxidation, STM measurements were performed before and after the reaction and insignificant changes in the surface morphology and roughness were found. Consequently, it appears that the Pt<sub>2</sub>Bi surface became kinetically stabilized due to the competition between the oxidation of formic acid at the electrode/solution interface and Bi leaching, *i.e.*, corrosion/oxidation processes of the electrode surface itself.<sup>79</sup> Accordingly, the main reasons for high stability of Pt<sub>2</sub>Bi catalyst is the suppression of Bi leaching, as well as inhibition of dehydration path in the reaction of formic acid oxidation.

On the other hand, the lower onset potential for HCOOH oxidation and higher reaction currents on Pt<sub>2</sub>Bi alloy compared to both Pt/Bi<sub>IRR</sub> electrodes were the result of ensembles that were created by alloyed Bi atoms incorporated

into the Pt lattice, causing a shift in the d-band center of the adjacent Pt atoms. Therefore, Bi in the alloy also exhibited an electronic effect, which could enhance the affinity towards HCOOH adsorption and thus increasing the interaction of HCOOH molecules with the catalyst surface.

It was found that all the investigated bimetallic catalysts were more active than Pt with the onset potentials shifted to more negative values and the currents at 0.0 V vs. SCE (under steady state conditions) improved by up to two order of magnitude (Table II).

TABLE II. Activity of the respective catalysts at  $E = 0.0$  V (SCE) determined under steady-state conditions

Activity parameter	Catalyst			
	Pt poly	Pt/Bi <sub>I<sub>RR</sub></sub> , $\theta \approx 0.3$	Pt/Bi <sub>I<sub>RR</sub></sub> , $\theta \approx 0.5$	Pt <sub>2</sub> Bi
$j / \text{mA cm}^{-2}$	0.0038	0.058	0.36	0.48
$j_{\text{Pt}_2\text{Bi}}/j_{\text{respective catalyst}}$	127	8.3	1.33	1

Comparison of the results obtained for these different bulk Pt–Bi catalysts indicated that Bi in the alloy and irreversibly adsorbed Bi exhibited different effects on the catalytic activity. This enables distinguishing between the role of the ensemble and electronic effects in the oxidation of formic acid on Pt–Bi electrodes. The electronic effect, existing only on the alloy, contributes to an earlier start of the reaction, while the maximum current originates from an ensemble effect. During potential cycling of the Pt/Bi<sub>I<sub>RR</sub></sub> electrode, Bi was leached from the electrode surface and the ensemble effect was reduced over time, or lost.

## 2.2. Stability of bulk catalysts

From a practical point of view, long-term stability of the investigated catalysts for the oxidation of formic acid is very important. The stabilities of the Pt–Bi catalysts were tested by chronoamperometric measurements and by prolonged potential cycling in the supporting solution as well as in the supporting solution containing formic acid. The aim of the study was to establish which factors mostly affected the improvement of the oxidation rate of formic acid and the stability of the catalyst. Additionally, a parallel study on a Pt electrode was performed to verify the promotional role of Bi.

Cyclic voltammograms recorded on Pt<sub>2</sub>Bi catalyst in the formic acid containing electrolyte are shown in Fig. 3. Over the potential cycling up to 0.8 V vs. SCE, the activity of Pt<sub>2</sub>Bi electrode slowly decreased during the first 5–7 cycles reaching values of  $\approx 85\%$  of the initial currents. After these first few sweeps, the currents remain unchanged with further cycling. On the contrary, the cycling of Pt<sub>2</sub>Bi in supporting electrolyte led to enhancement of the currents related to the oxidation of Bi species, indicating some surface decomposition caused by Bi leaching/dissolution process (Fig. 3, inset A). It appears, consequently, that sta-

bility of Pt<sub>2</sub>Bi during oxidation of formic acid could be induced by the presence of formic acid in the electrolyte.

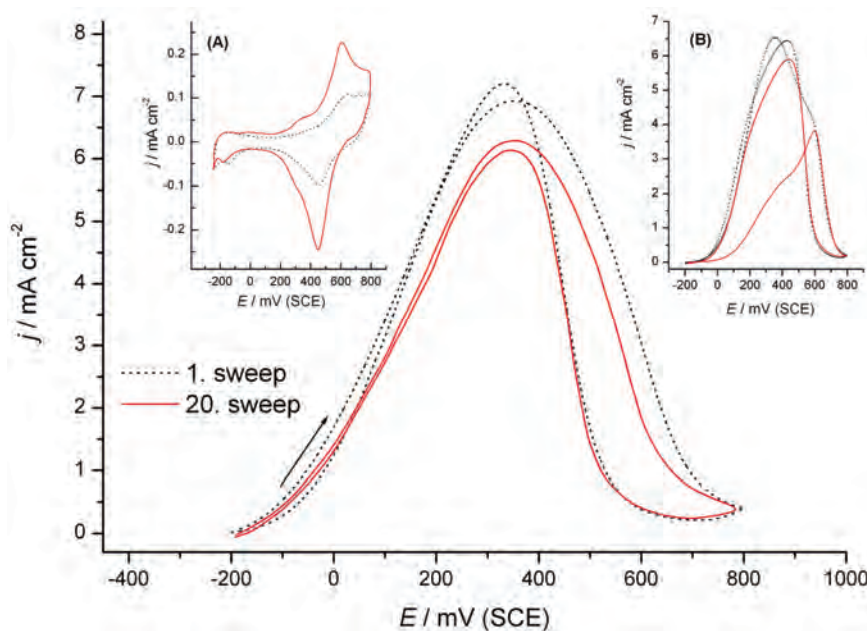


Fig. 3. Cyclic voltammograms (1<sup>st</sup> and 20<sup>th</sup> sweep) for the oxidation of 0.125 M HCOOH in 0.1 M H<sub>2</sub>SO<sub>4</sub> solution at a Pt<sub>2</sub>Bi catalyst. Insets: A) basic voltammograms (1<sup>st</sup> and 20<sup>th</sup> sweep) for Pt<sub>2</sub>Bi electrode in 0.1 M H<sub>2</sub>SO<sub>4</sub> solution and B) cyclic voltammograms (1<sup>st</sup> and 20<sup>th</sup> sweep) for the oxidation of 0.125 M HCOOH in 0.1 M H<sub>2</sub>SO<sub>4</sub> solution at Pt/Bi<sub>IRR</sub>;  $\theta=0.3$  electrode. Scan rate: 50 mV s<sup>-1</sup>.  $\omega=1500$  rpm.  $T=295$  K.

Contrary to the Pt<sub>2</sub>Bi catalyst, the Pt/Bi<sub>IRR</sub> electrode shows significant changes with continuous cycling in the solution containing formic acid (Fig. 3, inset B).<sup>72</sup> Repetitive cycling up to 0.8 V vs. SCE shifted the onset potential for formic acid oxidation to more positive values, decreased the reaction currents, while anodic peak diminished and a new peak starts to emerge and grow at  $\approx 0.6$  V vs. SCE. This transformation of the cyclic voltammograms indicated modification of the surface composition due to continuous Bi dissolution. Apparently, re-adsorption of Bi species from the solution was rather low, so the initial voltammogram was never restored, which is in accordance with results obtained for formic acid oxidation on bismuth-coated mesoporous Pt microelectrodes.<sup>80</sup>

To test the assumption that the presence of formic acid stabilizes the catalyst, a Pt<sub>2</sub>Bi electrode was subjected to potential cycling in the supporting electrolyte and after 20 cycles the electrode was replaced by a Pt electrode (Fig. 4a). The results of this experiment showed a slightly reduced charge of hydrogen adsorption/desorption indicating underpotential deposition of the previously leached/

/dissolved Bi. The same procedure was repeated in the electrolyte containing formic acid. The voltammogram of formic acid oxidation recorded on Pt in this experiment almost retraced the characteristic profile of pure Pt, suggesting that leaching of Bi was suppressed in the presence of formic acid. This was confirmed by STM measurements performed before and after the oxidation of formic acid, indicating a small difference in roughness and an insignificant change in the surface morphology.<sup>48</sup>

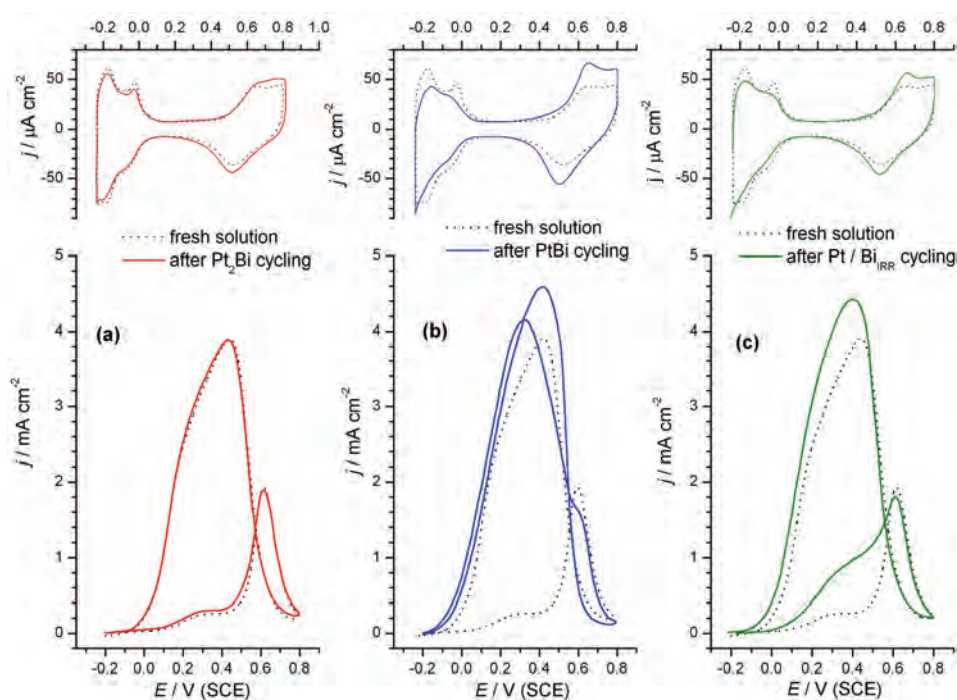


Fig. 4. Comparison of cyclic voltammograms recorded after replacement of: a) Pt<sub>2</sub>Bi, b) PtBi and c) Pt/Bi<sub>IRR</sub> with polycrystalline Pt in 0.1 M H<sub>2</sub>SO<sub>4</sub> solution and in 0.125 M HCOOH solution. Scan rate: 50 mV s<sup>-1</sup>.  $\omega = 1500$  rpm.  $T = 295$  K.

It should be noted that the experiment performed after replacing the PtBi alloy with Pt revealed significant Bi leaching under the same experimental conditions, meaning that Pt<sub>2</sub>Bi was more resistant to Bi leaching than PtBi (Fig. 4b). The same experiment conducted with the Pt/Bi<sub>IRR</sub> electrode showed considerable changes in surface composition due to Bi dissolution. Upon prolonged cycling, the electrode surface became enriched in platinum and exhibited a Pt-like electrochemical behavior in acid electrolyte containing formic acid (Fig 4c).

Although Pt/Bi<sub>IRR</sub> shows remarkable initial activity compared to pure Pt, this electrode was not stabilized by formic acid oxidation, since the desorption of Bi was not suppressed in the presence of formic acid. In addition, the poisoning



effect induced by the dehydration path was not avoided and  $\text{Bi}_{\text{IRR}}$  did not provoke any significant modification of the electronic environment. Therefore,  $\text{Pt}/\text{Bi}_{\text{IRR}}$  catalysts are less active than the corresponding alloy.

Chronoamperometric experiments were performed to prove the activity and stability of the investigated catalysts (Fig. 5). Insight into the chronoamperometric curves confirmed the advantage of alloys, *i.e.*, the necessity of alloying Pt with Bi to obtain a catalyst with stable activity.

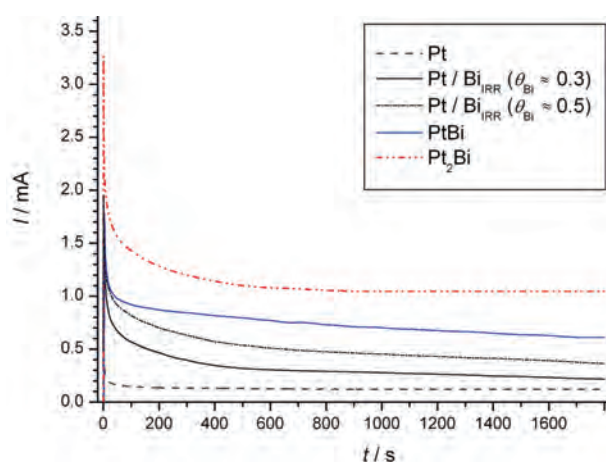


Fig. 5. Chronoamperometric curves for the oxidation of 0.125 M HCOOH at 0.2 V in 0.1 M  $\text{H}_2\text{SO}_4$  solution on PtBi,  $\text{Pt}_2\text{Bi}$ ,  $\text{Pt}/\text{Bi}_{\text{IRR}}$  and Pt catalysts.  $\omega = 1500$  rpm.  $T = 295$  K.

In summary, the main reason for the high stability of the  $\text{Pt}_2\text{Bi}$  catalyst is the inhibition of the dehydration path in the reaction, as well as suppression of Bi leaching in the presence of formic acid, which is specified by a minor change in the surface morphology and roughness.<sup>48,72</sup> Comparing the results obtained for the two types of Pt–Bi catalysts, polycrystalline Pt modified by irreversible adsorbed Bi and for  $\text{Pt}_2\text{Bi}$  catalyst, the role of the ensemble effect and electronic effect in the oxidation of formic acid was distinguished.<sup>48</sup> The electronic effect contributes to a lower onset potential of the reaction, while the maximum current comes from the ensemble effect. During the potential cycling treatment of the  $\text{Pt}/\text{Bi}_{\text{IRR}}$  electrode, Bi is dissolved from the electrode surface and the ensemble effect is reduced or lost over time. On the other hand, the high stability of the  $\text{Pt}_2\text{Bi}$  catalyst, confirmed by chronoamperometric experiments, proves an advantage of alloys, *i.e.*, the necessity of alloying Pt with Bi to obtain a corrosion resistant catalyst. According to Liu *et al.*,<sup>79</sup> the high stability of the PtBi intermetallic is due to suppressed leaching of Bi in the presence of formic acid because of the effective competition between oxidation of the organic molecule at the electrode surface and the corrosion/oxidation of the electrode surface itself.

### 3. LOW-LOADING Pt–Bi CATALYSTS

#### 3.1. Activity of low-loading catalysts

The concept of bimetallic mono and multilayer catalysts has received much attention regarding its possibility to reduce the noble metal loading and maintain the activity by replacing the under-layer (or bulk of the catalyst) with a less noble metal. In addition, unlike other bimetallic catalysts where the second metal is either in the form of an adatom or as a surface alloy component, this type of catalyst allows the study of the electronic effect of the second metal under-layer to the noble catalyst over-layer, as the only operating factor.

##### 3.1.1. Pt/GC catalyst

Pt was deposited onto a glassy carbon substrate (Pt/GC) using chronocoulometry at the potential corresponding to Pt limiting current plateau.<sup>70</sup> For the sake of comparison, a Pt/GC electrode was prepared using the same electrochemical procedure and the quantity analogous to one for a bimetallic electrode.

AFM imaging of the Pt deposit on the GC substrate showed randomly distributed clusters (agglomerates), which consisted of spherical nanoparticles with a regular size distribution of  $5.7 \pm 1.5$  nm, as revealed by STM measurements.<sup>70</sup>

Catalytic activity of Pt/GC electrode for formic acid oxidation was examined by potentiodynamic and quasi steady-state measurements. The reaction proceeds through both paths featured by higher first and lower second anodic, indicating lower poisoning of this Pt surface compared to the Pt bulk electrode and a shift in the reaction towards the direct path. STM analysis of this electrode revealed rather small, loosely packed particles with a diameter of  $\approx 5$  nm, which should have a lower number of defects and smaller Pt ensembles exposed to the reaction. Such morphology of the particles should lead to a more pronounced direct path in formic acid oxidation. These results are in accordance with a previously reported conclusion<sup>81</sup> that the particle structure, *i.e.*, morphology, rather than the particle size plays a predominant role in the activity of Pt catalysts for formic acid oxidation. The particle structure is directed by particle growth, which is influenced by the support morphology and saturation of the active centers of the support by a metal precursor.

##### 3.1.2. Pt@Bi/GC clusters

Formic acid oxidation was studied on a Pt–Bi catalyst obtained using an unusual approach for the preparation, *i.e.*, modification of the Bi deposit with a Pt overlayer.<sup>70</sup> Briefly, platinum–bismuth deposits on a glassy carbon (GC) rotating disk electrode were prepared by a two-step process. Electrochemical deposition of a controlled amount of Bi was performed at  $-0.1$  V *vs.* SCE onto a mirror-like polished GC substrate. Subsequently, the electrodes were rinsed and transferred to the solution for deposition of Pt. It should be stressed that Pt deposition was realized at a potential of  $-0.1$  V *vs.* SCE, which corresponded to the Pt limiting current plateau, in order to avoid any displacement reaction between Pt

and the less noble Bi and/or GC substrate. For the same reason, the GC and GC/Bi electrodes were immersed and pulled out from the solution for Pt deposition at  $-0.1$  V *vs.* SCE. The electrodes prepared in such manner, denoted as Pt@Bi/GC, were characterized by AFM spectroscopy, which indicated that Pt crystallized preferentially onto the previously formed Bi particles.

Analysis of the current *vs.* time transient responses demonstrated compliance with theoretical curves for progressive 3D nucleation<sup>82</sup> in all three cases, *i.e.*, for Bi deposition on a GC substrate, for Pt deposition on Bi/GC surface and Pt deposited alone on a GC support. The density of nuclei at saturation imply not only higher coverage of GC surface by Bi in comparison to Pt, but also that Pt could be better spread over Bi than over GC.

The issue of Bi leaching (dissolution) from PtBi catalysts, and their catalytic effect alongside the HCOOH oxidation is rather unresolved. In order to control Bi dissolution, as prepared electrode were subjected to electrochemical oxidation by slow sweep in the supporting electrolyte within the relevant potential range. Such oxidized electrodes are denoted as “treated Pt@Bi/GC”. This procedure led to quantitative oxidation of Bi partially occluded by Pt, but simultaneously to the formation of Bi oxide, accordingly creating a surface composed of Pt and Bi oxide.

The SEM micrographs of the as-prepared and treated Pt@Bi/GC electrodes are shown in Fig. 6a and b, respectively. The SEM image of the as-prepared sample shows well separated, randomly distributed clusters (agglomerates), with size of about 700 nm, which were formed from smaller particles. After electrochemical treatment of Pt@Bi agglomerates, the SEM image showed a decrease in the number and size of the isolated clusters, indicating some dissolution of uncovered/unprotected Bi deposit.

Anodic stripping charges indicated that along oxidation procedure about 70% of the quantity of deposited Bi was oxidized (Fig. 6c). The shape of the stripping peak implies the possibility of its deconvolution into two peaks, a sharp one that corresponds to Bi dissolution and a broader one at more positive potential that suits Bi oxide formation.<sup>83</sup> ICP mass spectroscopic analysis of the electrolyte after this electrochemical treatment revealed that Bi was only partially dissolved, which confirmed the possibility of the formation of some Bi oxide species.

These assumptions were confirmed by EDX spectra, which evidenced the presence of Pt, Bi and O, showing a decrease in Bi quantity in the Pt@Bi/GC electrode after the slow sweep and significant increase in the oxygen content, which may be attributed to Bi oxide formation (Fig. 6d). Thus, the composition of the treated Pt@Bi/GC obtained by EDX analysis corresponded qualitatively well to the results obtained by the deconvolution of the stripping peak.

In this way, the prepared electrode exhibited significantly high activity and exceptional stability in comparison to the Pt/GC electrode. Formic acid oxidation

proceeded predominantly through the dehydrogenation path on the treated Pt@Bi/GC electrode, resulting in its high activity. The onset potential was shifted by 150 mV to more negative values and the currents were about 10 times higher than those at the same potential on Pt/GC, as revealed both by potentiodynamic as well as by quasi-steady state measurements (Fig. 7).

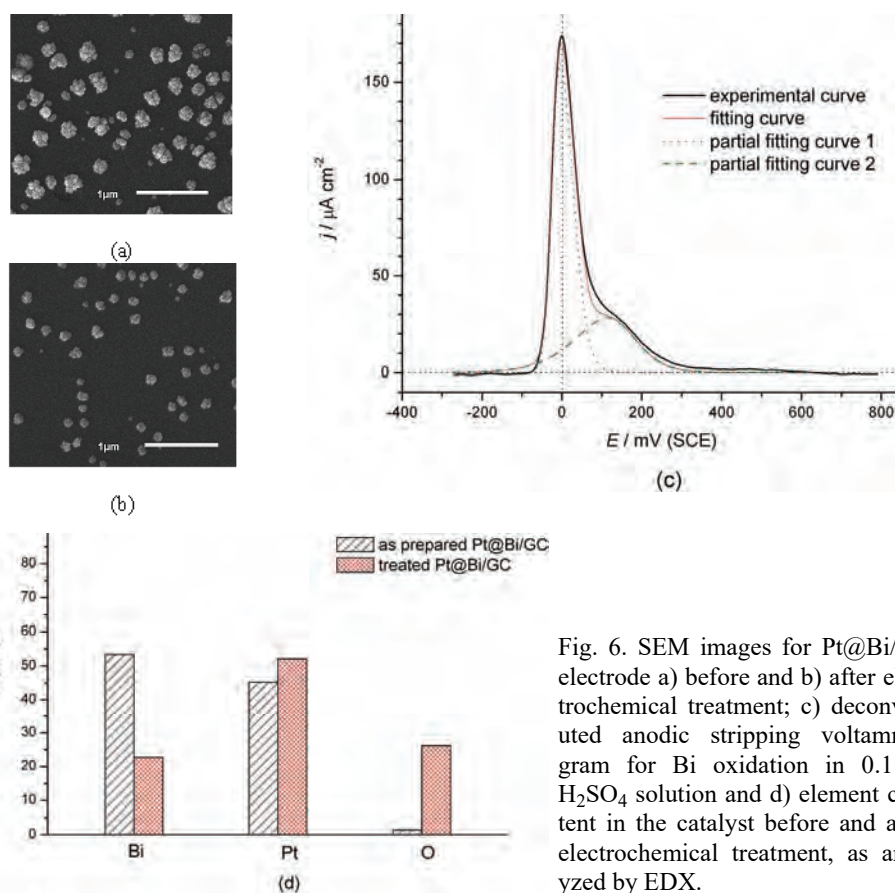


Fig. 6. SEM images for Pt@Bi/GC electrode a) before and b) after electrochemical treatment; c) deconvoluted anodic stripping voltammogram for Bi oxidation in 0.1 M H<sub>2</sub>SO<sub>4</sub> solution and d) element content in the catalyst before and after electrochemical treatment, as analyzed by EDX.

This high activity and increased selectivity toward dehydrogenation is the result of well-balanced ensemble effect originating from the interruption of continuous Pt sites by Bi-oxide domains. The possibility of some electronic effect of non-oxidized Bi under the Pt on the activity of the Pt@Bi/GC electrode could not be excluded. Prolonged cycling and chronoamperometry tests revealed exceptional stability of the catalyst during formic acid oxidation.<sup>70</sup> This low loading Pt-based electrode exhibited activity for the oxidation of formic acid similar to that of bulk Pt<sub>2</sub>Bi alloy, which has been shown to be one of the best Pt–Bi bimetallic catalysts for the oxidation of formic acid.<sup>48</sup>

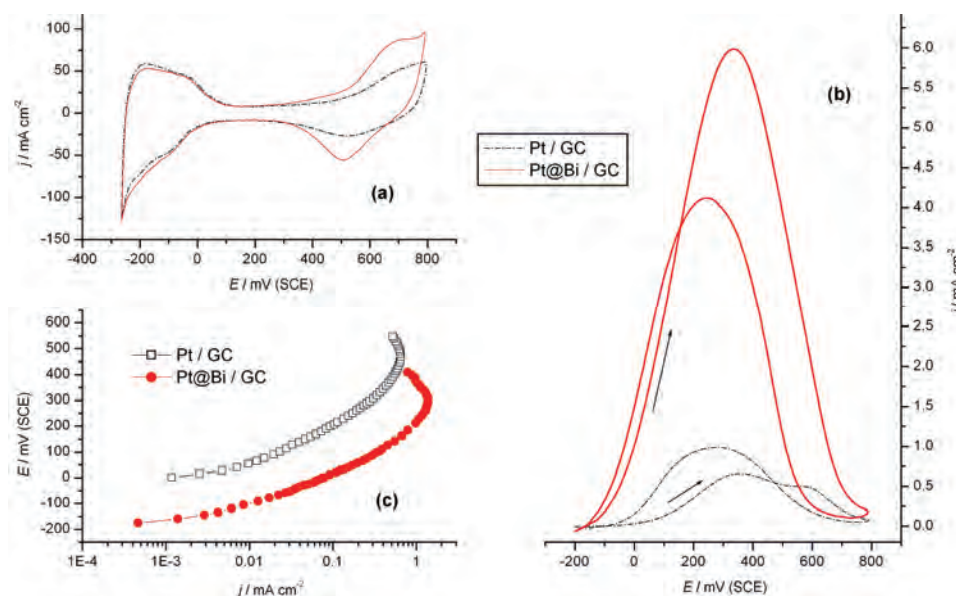


Fig. 7. Initial cyclic voltammograms: a) for treated Pt/GC and treated Pt@Bi/GC electrodes in 0.1 M  $\text{H}_2\text{SO}_4$  solution and b) for the oxidation of 0.125 M  $\text{HCOOH}$  in 0.1 M  $\text{H}_2\text{SO}_4$  solution (scan rate  $50 \text{ mV s}^{-1}$ ); c) corresponding Tafel plots (scan rate  $1 \text{ mV s}^{-1}$ ).  $\omega = 1500 \text{ rpm}$ .  $T = 295 \text{ K}$ .

### 3.2. Stability of low-loading catalysts

As already stated, upon treatment of as prepared Pt@Bi/GC clusters by a slow anodic sweep, a unique bimetallic structure consisting of a Bi core occluded by Pt and a Bi-oxide was obtained. Consideration of the stability of the Pt@Bi/GC catalyst was realized by applying prolonged potential cycling up to 0.8 V vs. SCE (hereinafter referred to as a cycling protocol) in supporting electrolyte or in supporting electrolyte containing formic acid and the results were compared with data obtained at a Pt/GC electrode treated in the same manner. An attempt was made to correlate the electrochemical response with the structural features of these two catalysts and to signify the effects that determine the electrode stability in formic acid oxidation.<sup>84</sup>

The difference in activity between Pt@Bi/GC and Pt/GC catalyst after the application of cycling protocol in appropriate electrolyte revealed a complex phenomenology, suggesting that the interplay of several factors, such as nanoparticle size, surface morphology, influence of formic acid and its intermediate  $\text{CO}_{\text{ads}}$ , determines the performance of the catalysts in formic acid oxidation.

Oxidation of  $\text{HCOOH}$  at the Pt@Bi/GC electrode occurred directly through dehydrogenation to  $\text{CO}_2$  enabled by the well-balanced Bi-oxide domains and small Pt ensembles, which resulted in remarkable stability of this catalyst. Seri-

ous formic acid oxidation effectively competes with oxidation of the electrode surface, *i.e.*, dissolution of Bi.<sup>79</sup> Leaching of Bi from Pt@Bi/GC in the presence of formic acid was not prevented but highly suppressed due to the source of Bi, *i.e.*, Bi core. Since this electrode is composed of a Bi core occluded by Pt and Bi oxide, the morphology of the surface slightly changes and facilitates high activity and stability of this catalyst.

Pt@Bi/GC catalyst exhibited excellent stability during prolonged oxidation of formic acid even above the potentials of Bi dissolution, as revealed by the negligible decrease in activity (Fig. 8a). Such stability of the catalyst was confirmed by quasi-steady state measurements performed on the surface previously treated by potential cycling in supporting electrolyte containing formic acid. The data obtained under slow sweep conditions corroborated the difference in the activities of investigated catalysts, as was found by the potentiodynamic measurements. These measurements also showed high selectivity of this surface toward the dehydrogenation path. Tafel slopes of 120 mV obtained at Pt@Bi/GC electrode after 1, 20 and 100 cycles in the supporting electrolyte containing formic acid indicate that the dehydrogenation path in formic acid oxidation proceeded on a surface free of adsorbed CO species. Contrary to the Pt@Bi/GC electrode, which possessed high stability and unusual cycling performance in formic acid oxidation, the activity of the Pt/GC electrode during the cycling protocol in the presence of formic acid in the supporting electrolyte continuously decreased (Fig. 8b). Even more, while at Pt@Bi/GC electrode, the reaction proceeded continuously through the direct path, in the case of Pt/GC, the reaction mechanism changes during cycling. As can be seen from Fig. 8b, in the first cycle, the current raises and reaches a peak that indicates predominant direct oxidation of HCOOH, while the appearance of a well-defined shoulder on the descending part of the curve signifies the indirect path in the reaction as well. As the number of cycles increases, the currents related to dehydrogenation diminish and simultaneously, the well-defined shoulder transforms into a peak, indicating the increased role of the indirect path in the reaction.

This decrease in the activity of Pt/GC electrode could not only be due to a gradual accumulation of reaction residues, *i.e.*, poisoning, on the electrode surface, but also to structural adjustments of the platinum nanoparticles as a result of the changes in the potentials during the scanning in acidic solutions, especially in the presence of the organic compound. The Tafel slope obtained for Pt/GC electrode of 140 mV (Fig. 8b) indicates that the reaction occurred on the surface partially covered by CO<sub>ads</sub>, not only through the dehydrogenation path, but also *via* the dehydration path occurring in parallel. Significant decreases in the currents and increases in the Tafel slope after 20 and 100 cycles indicate retardation of the reaction due to adsorption and accumulation of CO on the surface.

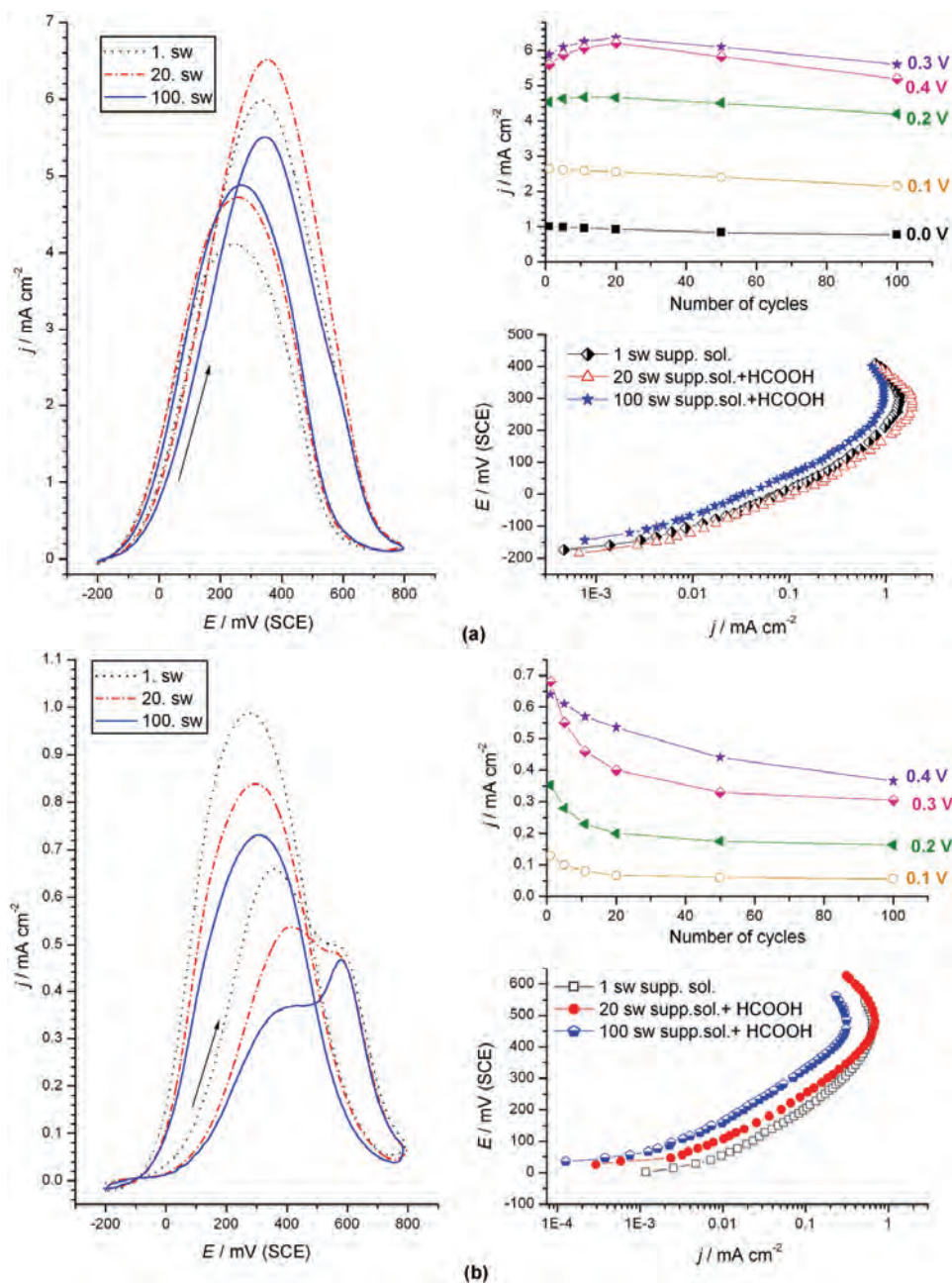


Fig. 8. Cyclic voltammograms for the oxidation of 0.125 M HCOOH in 0.1 M H<sub>2</sub>SO<sub>4</sub> (1<sup>st</sup>, 20<sup>th</sup> and 100<sup>th</sup> sweep at a rate of 50 mV s<sup>-1</sup>); effect of cycling – plots of current density vs. number of cycles and corresponding Tafel plots (scan rate 1 mV s<sup>-1</sup>) obtained a) on a Pt@Bi/GC electrode and b) on a Pt/GC electrode.  $\omega = 1500$  rpm.  $T = 295$  K.

The oxidation of adsorbed CO, usually used for surface characterization, was also employed to determine the electrochemically active surface area (*ECSA*) of a catalyst. The values calculated for Pt@Bi/GC and Pt/GC electrodes revealed that, regardless of the presence or absence of HCOOH in the supporting electrolyte, the *ECSA* of the Pt@Bi/GC electrode increased during the cycling protocol, while the *ECSA* decreased for the Pt/GC electrode (Fig. 9). However, the degree of *ECSA* change upon cycling for both electrodes significantly depended on whether the supporting electrolyte contained HCOOH. The *ECSA* of the Pt@Bi/GC electrode slightly increased during this treatment in presence of formic acid due to some Bi dissolution and was confirmed in the experiments with polycrystalline Pt (Fig. 10b).

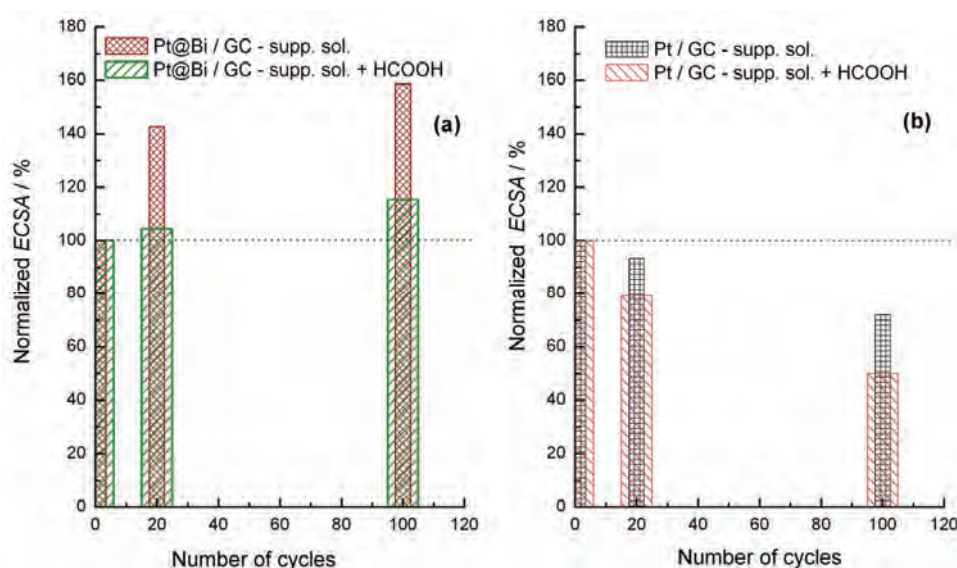


Fig. 9. Normalized *ECSA* values calculated with CVs upon potential cycling in supporting solution and in supporting solution containing 0.125 M HCOOH on: a) Pt@Bi/GC and b) Pt/GC electrodes. The normalized *ECSA* values were calculated by dividing the *ECSA* value after a certain number of potential cycles by that of the first cycle.

However, when this electrode was cycled in pure supporting electrolyte, the *ECSA* value increased significantly during the treatment (Fig. 9) because of intense leaching of Bi from the electrode, which was confirmed by the experiment with polycrystalline Pt (Figs. 10a and b).

On the other hand, the Pt/GC electrode exhibited completely opposite properties upon similar treatment in the supporting electrolyte with or without formic acid. When this electrode was subjected to potential cycling in the absence of HCOOH, the *ECSA* value decreased slightly (Fig. 9), which was primarily due to the coalescence and agglomeration of the particles. Some negli-



gible dissolution of Pt could also be possible.<sup>85</sup> The result of these phenomena was the formation of defects on the surface that led to some negative shift of the onset and the peak potential of the oxidation of  $\text{CO}_{\text{ads}}$ , which indicates a slight change in the surface morphology had occurred. The consequence of these minor surface alternations was a small decrease in the activity for the oxidation of formic acid.

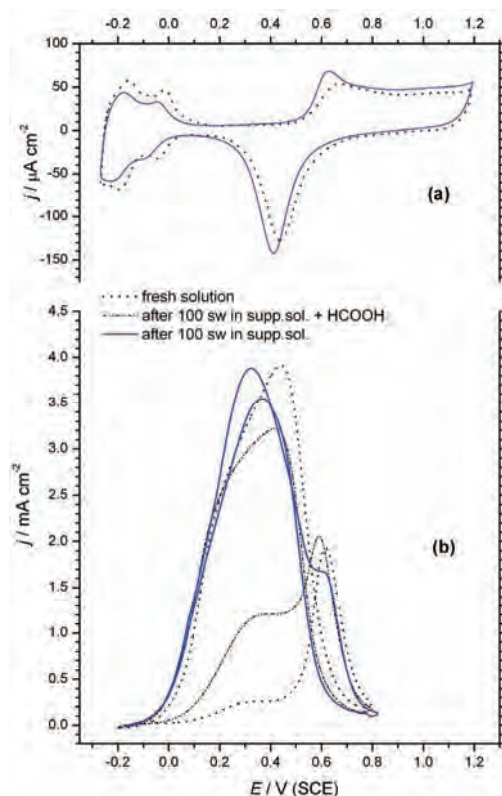


Fig. 10. Cyclic voltammograms recorded a) after replacement of Pt@Bi/GC that has been exposed to cycling protocol with a polycrystalline Pt electrode in 0.1 M  $\text{H}_2\text{SO}_4$  solution and b) for the oxidation of 0.125 M HCOOH in 0.1 M  $\text{H}_2\text{SO}_4$ . Scan rate:  $50 \text{ mV s}^{-1}$ .  $\omega = 1500 \text{ rpm}$ .  $T = 295 \text{ K}$ .

Furthermore, when the Pt/GC electrode was similarly treated in the presence of HCOOH, the ECSA decreased much more (Fig. 9) and a larger shift of the  $\text{CO}_{\text{ads}}$  stripping peaks in the negative direction was observed, indicating to a considerable perturbation in the surface morphology. The consequence of these changes was a significantly lower activity of these surfaces. Considering that formic acid oxidation proceeds on a Pt/GC electrode through both the direct dehydrogenation and the indirect dehydration path, and that during cycling the reaction turns more to the latter one in which CO adsorbs on the surface, it seems that adsorption of CO and its oxidation contribute not only to particle agglomeration but even more to Pt dissolution.

High stability of Pt@Bi/GC electrode is confirmed in chronoamperometric experiment (Fig. 11). Current density recorded on treated Pt@Bi/GC during 1800 s at a constant potential of 0.2 V was again significantly higher than on the Pt/GC electrode. At Pt/GC electrode, the current decayed rapidly reaching a low steady state value within a few minutes. Contrarily, the current decreased slowly at the Pt@Bi/GC electrode and stabilized at a value that was more than 10 times higher than for the other electrode. This experiment also demonstrated the higher stability of the Pt@Bi/GC electrode in comparison to the Pt<sub>2</sub>Bi catalyst<sup>48</sup> since under the same conditions, the decrease in the currents for HCOOH oxidation at the Pt@Bi/GC electrode was much lower compared to the decrease registered for the Pt<sub>2</sub>Bi catalyst.

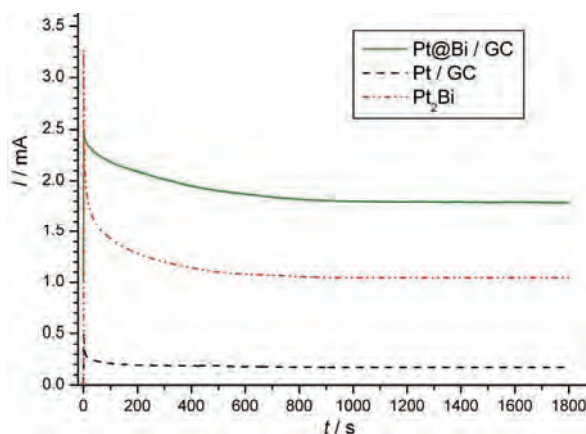


Fig. 11. Chronoamperometric curves for the oxidation of 0.125 M HCOOH in 0.1 M H<sub>2</sub>SO<sub>4</sub> solution at 0.2 V on Pt@Bi/GC and Pt/GC electrodes.  $\omega = 1500$  rpm.  $T = 295$  K.

### 3.3. Pt(Bi)/GC shell–core catalyst

The bimetallic PtBi electrodes, as catalysts for formic acid oxidation, were examined in terms of obtaining a steady state electrode surface. The catalyst, denoted as Pt(Bi)/GC was produced using a similar methodology of preparation as previously described for the Pt@Bi/GC catalyst, *i.e.*, by sequential deposition of Bi followed by deposition of Pt. In contrast to the experiments to test the stability of the Pt@Bi/GC catalyst, when its activation was performed by two slow sweeps up to 0.8 V *vs.* SCE, the Pt(Bi)/GC electrodes after metal deposition were activated by cycling the potential at a scan rate of 50 mV s<sup>-1</sup> between hydrogen and oxygen evolution (-0.27 up to 1.2 V *vs.* SCE) in 0.1 M H<sub>2</sub>SO<sub>4</sub> solution, prior to use as catalysts for the oxidation of formic acid. Generally, potential cycling is an electrochemical treatment that determines the degree of surface reconstruction and the size of the electrochemically active area. In the case of the Pt(Bi)/GC electrodes, this treatment was applied to quantify the amount of remaining Bi and Bi oxide in order to explain the importance of the composition and morphology of the surface for the reaction of formic acid oxidation.<sup>86</sup>

EDX and ICP-MS analysis, and AFM and electrochemical characterization, revealed that initially unfinished core-shell structures were formed. AFM characterization of the electrode surface indicated that Pt was preferentially deposited on the previously formed Bi particles, but cyclic voltammetry revealed leaching of Bi, meaning that Bi was not completely occluded by Pt.

The Pt(Bi)/GC catalysts were not stable at potentials beyond 0.4 V vs. SCE due to Bi leaching/dissolution from the surface, which occurred through the oxidation of the less-noble metal. Electrochemical treatment by potential cycling of the as-prepared electrode (Fig. 12a) led to quantitative oxidation of Bi from the

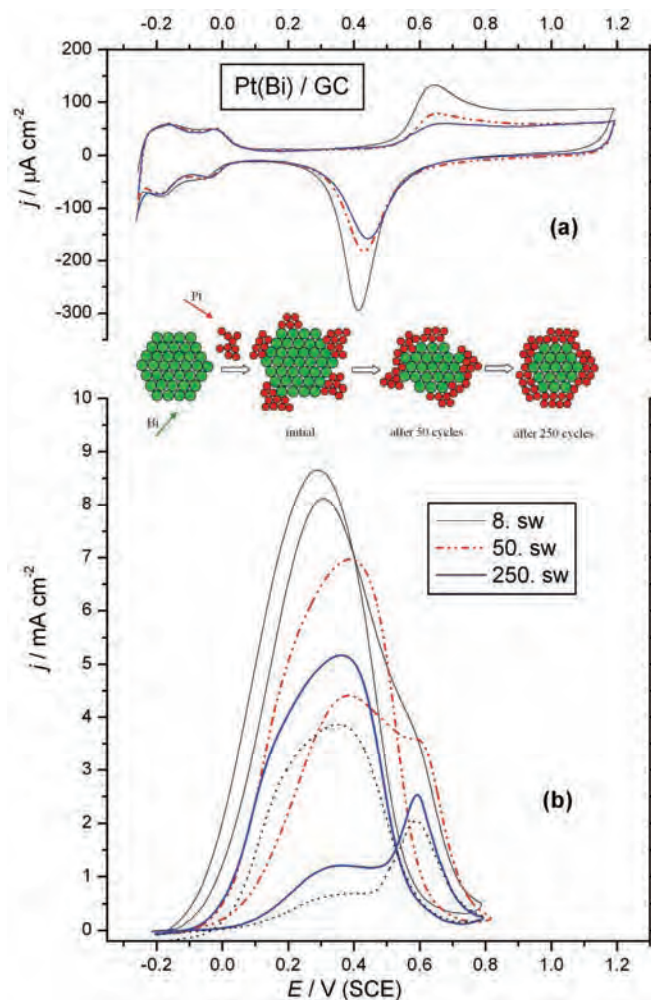


Fig. 12. Cyclic voltammograms recorded on the Pt(Bi)/GC electrode: a) in 0.1 M H<sub>2</sub>SO<sub>4</sub> and b) for the oxidation of 0.125 M HCOOH in 0.1 M H<sub>2</sub>SO<sub>4</sub> after 8, 50 and 250 cycles. Scan rate: 50 mV s<sup>-1</sup>.  $\omega = 1500$  rpm.  $T = 295$  K.

unprotected core and the simultaneous formation of Bi oxide, consequently creating a shell composed of Pt and Bi-oxide. By prolonged cycling, the amount of surface oxides diminished creating finally a Pt@Bi shell–core structure.

These electrodes exhibit enhanced electrocatalytic activity in formic acid oxidation in comparison to Pt/GC electrode treated in the same manner (Fig. 12b). This behavior could be explained primarily by an ensemble effect induced by surface Bi oxides interrupting the Pt domains, but to some extent, could also be attributed to the influence of the under-lying Bi onto the Pt surface layer, affecting the extent of poison adsorption on the Pt.

Electronic modification of Pt both by surface and sub-surface Bi can play some role as well. Significantly prolonged potential cycling in supporting electrolyte of Pt(Bi)/GC electrodes previously stabilized by Bi oxide led to considerably lower Bi leaching and was accompanied by dissolution and redeposition of Pt, resulting in a Pt shell over a Bi core. The Pt@Bi/GC (shell–core) catalysts, with only Pt in the surface layer exhibit somewhat enhanced activity due to the electronic effect of the remaining under-lying Bi, which depended on the thickness of the Pt layer determined by the quantity of Bi in the core. This observation was confirmed by results obtained at three catalysts with different ratio of Pt and Bi (different underlying thickness of Bi).<sup>86</sup>

In this way, by controlling the thickness of the Bi and Pt layers using electrochemical techniques, it was possible to improve the electrocatalytic properties of Pt(Bi)/GC in HCOOH oxidation and to create a low-loaded Pt-based catalyst with comparable activity to that of the bulk metal alloy.

#### 4. CONCLUSIONS

According to the results presented in this work dealing with the effects influencing the overall formic acid oxidation, it was found that both types of Pt–Bi bimetallic catalysts (bulk and low-loaded deposits on GC) showed superior catalytic activity compared to Pt, in terms of the lower onset potential and higher oxidation current density. Both types of Pt–Bi catalysts were investigated in order to establish how Bi atoms affect the adsorption characteristics of Pt towards formic acid.

It was found that among all the tested Pt–Bi bimetallic bulk catalysts, Pt<sub>2</sub>Bi is the most powerful for formic acid oxidation, exhibiting high activity and stability. High activities of the bulk bimetallic catalysts result from the fact that formic acid oxidation proceeds completely through the dehydrogenation path. Increased selectivity toward dehydrogenation is caused by an ensemble effect. The high stability of Pt<sub>2</sub>Bi surfaces are induced by the suppression of Bi leaching, as was evidenced by the insignificant changes in the morphology and roughness of the surfaces before and after electrochemical treatment in formic acid containing solution. The results presented indicate that Bi in alloy and irreversibly adsorbed

Bi exhibit different effects on the catalytic activity. Bi in the alloy not only induces an ensemble effect, but also has an electronic effect, which could be the reason for better performance of this catalyst resulting in higher currents and a lower onset potential. The activity of PtBi alloy is caused by UPD phenomena of Bi on Pt, which was electrochemically detected. In addition, based on XPS analysis, it is proposed that the activity of PtBi could also be caused by the bifunctional action of hydroxylated Bi species.

Comparing the results obtained for these bulk Pt–Bi catalysts, the role of the ensemble effect and electronic effect in the oxidation of formic acid could be distinguished. The electronic effect, existing only on the alloy, contributed to the earlier start of the reaction, while the enhanced maximum current originates from the ensemble effect. Thus, the stability of the catalytic activity of Pt–Bi bimetallic electrodes is strongly related to the leaching tolerance of the electrode surface during formic acid oxidation. The leaching tolerance of anodic catalysts was greatly enhanced by the formation of alloy between Pt and Bi, *i.e.*, it is necessary to alloying Pt with Bi to obtain a corrosion stable bulk catalyst.

Electrochemical deposition of low loading Pt layer over Bi deposits on a GC electrode resulted in the formation of approximately spherical clusters of Bi covered by Pt. Treatment of the as-prepared electrode in the relevant potential range and supporting electrolyte leads to quantitative oxidation of Bi partially occluded by Pt, and simultaneously to the formation of Bi oxide, thus creating a surface composed of Pt and Bi-oxide. The so-prepared electrode exhibits higher activity and exceptional stability in comparison to a pure Pt/GC electrode. Formic acid oxidation proceeds predominantly through dehydrogenation path on treated Pt@Bi/GC electrode resulting in its high activity. The increased selectivity toward dehydrogenation is caused by an ensemble effect originating from the interruption of continuous Pt sites by Bi-oxide domains. The possibility of some electronic effect of non-oxidized Bi under the Pt on the activity of Pt@Bi/GC cannot be excluded. Such stability is induced by the stability of the Bi-oxide formed during electrode pre-treatment. This low loading Pt-based electrode exhibits activity for the oxidation of formic acid similar to the activity of bulk Pt<sub>2</sub>Bi alloy, which has been shown to be one of the best Pt–Bi bimetallic catalysts for the oxidation of formic acid.

The use of bimetallic compounds as anode catalysts is an effective solution to overcome the problems with stability of the formic acid oxidation current for long-term applications. In the future, the tolerance of both CO poisoning and electrochemical leaching should be considered as the key factors in the development of electrocatalysts for anodic reactions.

*Acknowledgement.* This work was financially supported by the Ministry of Education, Science and Technological Development of the Republic of Serbia, Contract No. H-172060.

## ИЗВОД

## ОКСИДАЦИЈА МРАВЉЕ КИСЕЛИНЕ НА КАТАЛИЗАТОРИМА ПЛАТИНА–БИЗМУТ

КСЕНИЈА Ђ. ПОПОВИЋ и ЈЕЛЕНА Д. ЛОВИЋ

*ИХТМ – Центар за електрохемију, Универзитет у Београду, Њевошева 12, п. бр. 473, 11000 Београд*

Електрохемијска оксидација мравље киселине је предмет истраживања последњих деценија као модел реакција за разумевање механизма оксидације малих органских молекула, као и због њене могуће примене у горивним спреговима. Платина је један од најчешће коришћених катализатора за ову реакцију упркос томе што показује неколико значајних недостатака који спречавају њену широку практичну примену: има високу цену и показује врло изражен пад ефикасности услед тровања површине адсорбованим интермедијерима ( $\text{CO}_{\text{ads}}$ ). Да би се превазишли ови проблеми и побољшале каталитичка својства катализатора, платина се модификује другим металима, па се стога све више користе биметални платински катализатори. Посебна пажња је усмерена на  $\text{Vi}$  као модификатор платине. Оксидација мравље киселине испитивана је на два типа  $\text{Pt-Vi}$  електрода: на масивним електродама и на електродама добијеним таложењем танких филмова на носаче од стакластог угљеника. Оба типа биметалних катализатора показују знатно већу активност и изузетну стабилност у поређењу са чистом  $\text{Pt}$ . Резултати приказани у овом прегледу значајни су за разумевање механизма електрооксидације мравље киселине на легурама  $\text{Pt-Vi}$  и  $\text{Pt}$  модификованој бизмутом, за развој нових анода побољшаних карактеристика за примену у горивим спреговима са мрављом киселином као горивом (DFAFC), као и за синтезу биметалних катализатора са малим садржајем  $\text{Pt}$  на бази танких филмова. Коришћењем ових биметалних катализатора превазишао би се и проблем стабилности анодног материјала за дугорочну примену у горивним спреговима.

(Примљено 18. марта, ревидирано 24. априла, прихваћено 5. маја 2015)

## REFERENCES

1. R. Parsons, T. Van der Noot, *J. Electroanal. Chem.* **257** (1988) 9
2. X. Wang, J.-M. Hu, I.-M. Hsing, *J. Electroanal. Chem.* **562** (2004) 73
3. J. Willsau, J. Heitbaum, *Electrochim. Acta* **31** (1986) 943
4. X. Yu, P. G. Pickup, *J. Power Sources* **182** (2008) 124
5. C. Rice, S. Ha, R. I. Masel, A. Wieckowski, *J. Power Sources* **111** (2002) 83
6. M. W. Breiter, *Electrochim. Acta* **8** (1963) 447
7. T. D. Jarvi, E. M. Stuve, in *Electrocatalysis*, J. Lipkovski, P. N. Ross, Eds., Wiley-VCH, New York, 1998, pp. 75–154
8. T. J. Schmidt, R. J. Behm, B. N. Grgur, N. M. Marković, P. N. Ross, *Langmuir* **16** (2000) 8159
9. J. M. Feliu, E. Herrero, in: *Handbook of Fuel Cells-Fundamentals Technology and Applications, Vol. 2: Electrocatalysis*, W. Vielstich, A. Lamm, H.A. Gasteiger (Eds.), John Wiley & Sons Ltd., Chichester, 2003, pp. 625–634
10. S. Park, Y. Xie, M. J. Weaver, *Langmuir* **18** (2002) 5792
11. E. Levina, T. Iwasita, E. Herrero, J. M. Feliu, *Langmuir* **13** (1997) 6287
12. N. M. Marković, P. N. Ross Jr., *Surf. Sci. Rep.* **45** (2002) 117
13. A. Boronat-González, E. Herrero, J. M. Feliu, *J. Solid State Electrochem.* **18** (2014) 1181
14. N. V. Rees, R. G. Compton, *J. Solid State Electrochem.* **15** (2011) 2095
15. A. Capon, R. Parsons, *J. Electroanal. Chem.* **44** (1973) 1
16. A. Capon, R. Parsons, *J. Electroanal. Chem.* **45** (1973) 205

17. J. Clavilier, R. Parsons, R. Durand, C. Lamy, J. M. Leger, *J. Electroanal. Chem.* **124** (1981) 321
18. R. R. Adžić, A. Tripković, V. B. Vešović, *J. Electroanal. Chem.* **204** (1986) 329
19. A. Tripković, K. Popović, *J. Serb. Chem. Soc.* **60** (1995) 297
20. A. Tripković, K. Popović, R. Adžić, *J. Chim. Phys.* **88** (1991) 1635
21. T. Iwasita, X. Xia, E. Herrero, H. D. Liess, *Langmuir* **12** (1996) 4260
22. G. Samjeske, A. Miki, S. Ye, M. Osawa, *J. Phys. Chem., B* **110** (2006) 16559
23. M. F. Mrozek, H. Luo, M. J. Weaver, *Langmuir* **16** (2000) 8463
24. A. Cuesta, G. Cabello, C. Gutierrez, M. Osawa, *Phys. Chem. Chem. Phys.* **13** (2011) 20091
25. C. Lamy, J. M. Leger, *J. Chim. Phys.* **88** (1991) 1649
26. V. Grozovski, F. J. Vidal-Iglesias, E. Herrero, J. M. Feliu, *ChemPhysChem* **12** (2011) 1641
27. H. Okamoto, Y. Numata, T. Gojuki, Y. Mukoyama, *Electrochim. Acta* **116** (2014) 263
28. A. Miki, S. Ye, M. Osawa, *Chem. Commun.* (2002) 1500
29. S.-C. Chang, L.-W. H. Leung, M. J. Weaver, *J. Phys. Chem. B* **94** (1990) 6013
30. P. K. Babu, H. S. Kim, J. H. Chung, E. Oldfield, A. Wieckowski, *J. Phys. Chem. B* **108** (2004) 20228
31. R. Adžić, A. V. Tripković, N. Marković, *J. Electroanal. Chem.* **150** (1983) 79
32. R. R. Adžić, in *Advances in Electrochemistry and Electrochemical Engineering*, H. Gerischer, C. W. Tobias, Eds., Wiley, New York, 1984, p. 159
33. N. de-los-Santos-Alvarez, L. R. Alden, E. Rus, H. Wang, F. J. Di Salvo, H. D. Abruna, *J. Electroanal. Chem.* **626** (2009) 14
34. L. J. Zhang, Z. Y. Wang, D. G. Xia, *J. Alloy. Compd.* **426** (2006) 268
35. W. Liu, J. Huang, *J. Power Sources* **189** (2009) 1012
36. Z. Awaludin, T. Okajima, T. Ohsak, *Electrochem. Comm.* **31** (2013) 100
37. O. Winjobi, Z. Zhang, C. Liang, W. Li, *Electrochim. Acta* **55** (2010) 4217
38. W. Chen, J. Kim, S. Sun, S. Chen, *Langmuir* **23** (2007) 11303
39. A. V. Tripković, K. Dj. Popović, R. M. Stevanović, R. Socha, A. Kowal, *Electrochem. Comm.* **8** (2006) 1492
40. J. Clavilier, A. Fernandez-Vega, J. M. Feliu, A. Aldaz, *J. Electroanal. Chem.* **258** (1989) 89
41. M. Ball, C. A. Lucas, N. M. Marković, B. M. Murphy, P. Steadman, T. J. Schmidt, V. Stamenković, P. N. Ross, *Langmuir* **17** (2001) 5943
42. D. Volpe, E. Casado-Rivera, L. Alden, C. Lind, K. Hagerdon, C. Downie, C. Korzniewski, F. J. Di Salvo, H. D. Abruna, *J. Electrochem. Soc.* **151** (2004) A971
43. H. Wang, L. Alden, F. J. Di Salvo, H. D. Abruna, *Phys. Chem. Chem. Phys.* **10** (2008) 3739
44. C. Roychowdhury, F. Matsumoto, V. B. Zeldovich, S. C. Warren, P. F. Mutolo, M. J. Ballesteros, U. Wiesner, H. D. Abruna, F. J. Di Salvo, *Chem. Mater.* **18** (2006) 3365
45. E. Casado-Rivera, D. J. Volpe, L. Alden, C. Lind, C. Downie, T. Vazquez-Alvarez, A. C. D. Angelo, F. J. Di Salvo, H. D. Abruna, *J. Am. Chem. Soc.* **126** (2004) 4043
46. J. Sanabria-Chinchilla, H. Abe, F. J. Di Salvo, H. D. Abruna, *Surf. Sci.* **602** (2008) 1830
47. E. Herrero, A. Fernandez-Vega, J. M. Feliu, A. Aldaz, *J. Electroanal. Chem.* **350** (1993) 73
48. J. D. Lović, M. D. Obradović, D. V. Tripković, K. Dj. Popović, V. M. Jovanović, S. Lj. Gojković, A. V. Tripković, *Electrocatalysis* **3** (2012) 346
49. X. Yu, P. G. Pickup, *Electrochim. Acta* **56** (2011) 4037

50. S. Daniele, S. Bergamin, *Electrochem. Comm.* **9** (2007) 1388
51. B.-J. Kim, K. Kwon, C. K. Rhee, J. Han, T.-H. Lim, *Electrochim. Acta* **53** (2008) 7744
52. S. R. Branković, J. X. Wang, R. R. Adžić, *Surf. Sci. Lett.* **747** (2001) L173
53. S. Papadimitriou, S. Armyanov, E. Valova, A. Hubin, O. Steenhaut, E. Pavlidou, G. Kokkinidis, S. Sotiropoulos, *J. Phys. Chem., C* **114** (2010) 5217
54. R. G. Freitas, E. C. Pereira, *Electrochim. Acta* **55** (2010) 7622
55. R. G. Freitas, E. P. Antunes, E. C. Pereira, *Electrochim. Acta* **54** (2009) 1999
56. A. Tegou, S. Papadimitriou, G. Kokkinidis, S. Sotiropoulos, *J. Solid State Electrochem.* **14** (2010) 175
57. S. Motoo, N. Furuya, *Ber. Bunsenges. Phys. Chem.* **91** (1987) 457
58. R. Carbo, R. Albalat, J. Claret, J. M. Feliu, *J. Electroanal. Chem.* **446** (1998) 79
59. J. M. Feliu, A. Fernandez-Vega, J. M. Orts, A. Aldaz, *J. Chim. Phys.* **88** (1991) 1493
60. S. P. E. Smith, H. D. Abruna, *J. Electroanal. Chem.* **467** (1999) 43
61. S. P. E. Smith, K. F. Ben-Dor, H. D. Abruna, *Langmuir* **15** (1999) 7325
62. J. Clavilier, A. Fernandez-Vega, J. M. Feliu, A. Aldaz, *J. Electroanal. Chem.* **261** (1989) 113
63. A. Sáez, E. Expósito, J. Solla-Gullón, V. Montiel, A. Aldaz, *Electrochim. Acta* **63** (2012) 105
64. A. Lopez-Cudero, F. J. Vidal-Iglesias, J. Solla-Gullon, E. Herrero, A. Aldaz, J. M. Feliu, *Phys. Chem. Chem. Phys.* **11** (2009) 416
65. J. Clavilier, J. M. Feliu, A. Aldaz, *J. Electroanal. Chem.* **243** (1988) 419
66. J. Kim, C. K. Rhee, *Electrochem. Comm.* **12** (2010) 1731
67. Q.-S. Chen, Z.-Y. Zhou, F. J. Vidal-Iglesias, J. Solla-Gullon, J. M. Feliu, S.-G. Sun, *J. Am. Chem. Soc.* **133** (2011) 12930
68. C. Jung, T. Zhang, B.-J. Kim, J. Kim, C. K. Rhee, T.-H. Lim, *Bull. Korean Chem. Soc.* **31** (2010) 1543
69. E. Casado-Rivera, Z. Gal, A. C. D. Angelo, C. Lind, F. J. Di Salvo, H. D. Abruna, *ChemPhysChem.* **4** (2003) 193
70. J. D. Lović, S. I. Stevanović, D. V. Tripković, V. V. Tripković, R. M. Stevanović, K. Dj. Popović, V. M. Jovanović, *J. Electrochem. Soc.* **161** (2014) H547
71. L. R. Alden, D. K. Han, F. Matsumoto, H. D. Abruna, F. J. Di Salvo, *Chem. Mater.* **18** (2006) 5591
72. J. D. Lović, D. V. Tripković, K. Dj. Popović, V. M. Jovanović, A. V. Tripković, *J. Serb. Chem. Soc.* **78** (2013) 1189
73. R. Gomez, J. M. Feliu, A. Aldaz, *Electrochim. Acta* **42** (1997) 1675
74. T. J. Schmidt, B. N. Grgur, R. J. Behm, N. M. Marković, P. N. Ross Jr., *Phys. Chem. Chem. Phys.* **2** (2000) 4379
75. S. Uhm, Y. Yun, Y. Tak, J. Lee, *Electrochem. Comm.* **7** (2005) 1375
76. M. Oana, R. Hoffmann, H. D. Abruna, F. J. Di Salvo, *Surf. Sci.* **574** (2005) 1
77. N. Kapur, B. Shan, J. Hyun, L. Wang, S. Yang, J. B. Nicholas, K. Cho, *Mol. Simulat.* **37** (2011) 648
78. V. Pautienienė, L. Tamašauskaitė-Tamašiūnaitė, A. Sudavičius, G. Stalnionis, Z. Jusys, *J. Solid State Electrochem.* **14** (2010) 1675.
79. Y. Liu, M. A. Lowe, F. J. Di Salvo, H. D. Abruna, *J. Phys. Chem., C* **114** (2010) 14929
80. S. Daniele, C. Bragato, D. Battistel, *Electroanalysis* **24** (2012) 759
81. D. Tripković, S. Stevanović, A. Tripković, A. Kowal, V. M. Jovanović, *J. Electrochem. Soc.* **155** (2008) B281



82. F. Gloaguen, J. M. Leger, C. Lamy, A. Marmanna, U. Stimming, R. Vogel, *Electrochim. Acta* **44** (1999) 1805
83. W. S. Li, X. M. Long, J. H. Yan, J. M. Nan, H. Y. Chen, Y. M. Wu, *J. Power Sources* **158** (2006) 1096.
84. J. D. Lović, S. I. Stevanović, D. V. Tripković, A. V. Tripković, R. M. Stevanović, V. M. Jovanović, K. Dj. Popović, *J. Solid State Electrochem* **19** (2015) 2223
85. L. Tang, B. Han, K. Persson, C. Friesen, T. He, K. Sieradzki, G. Ceder, *J. Am. Chem. Soc.* **132** (2010) 596
86. J. D. Lović, S. I. Stevanović, D. V. Tripković, V. M. Jovanović, R. M. Stevanović, A. V. Tripković, K. Dj. Popović, *J. Electroanal. Chem.* **735** (2014) 1.